Journal of Luminescence 200 (2018) 248–253

Contents lists available at ScienceDirect

Journal of Luminescence

journal homepage: www.elsevier.com/locate/jlumin

Optically stimulated luminescence of the [20% Li_2CO_3 + x% K_2CO_3 + (80 - x)% B_2O_3] glass system

João V.B. Valença[a,*], Anielle C.A. Silva[b], Noelio O. Dantas[b], Linda V.E. Caldas[c], Francesco d'Errico[d,e], Susana O. Souza[a]

[a] Universidade Federal de Sergipe, Departamento de Física, Av. Marechal Rondon, s/n – Jd. Rosa Elze, 50740-540 São Cristóvão, SE, Brazil
[b] Universidade Federal de Uberlândia, Instituto de Física, Laboratório de Novos Materiais Isolantes e Semicondutores (LNMIS), Uberlândia, MG, Brazil
[c] Instituto de Pesquisas Energéticas e Nucleares, Comissão Nacional de Energia Nuclear, IPEN-CNEN, São Paulo, Brazil
[d] Università di Pisa, Scuola di Ingegneria, Largo L. Lazzarino 2, Pisa I-56122, Italy
[e] Yale University, School of Medicine, PO Box 208042, New Haven, CT 06520-8042, United States

ARTICLE INFO

Keywords:
Borate glass
OSL
Thermal treatment

ABSTRACT

This study analyzed the optically simulated luminescence (OSL) of borate glasses containing lithium carbonate and potassium carbonate. Borate glasses present desirable characteristics for dosimetry and have been extensively analyzed in relation to thermoluminescence (TL). Five formulations containing 20% of Li_2CO_3 and different amounts of B_2O_3 and K_2CO_3 were produced. Their OSL signal was analyzed following exposure to beta particles. The decay pattern typical of continuous wave stimulation (CW-OSL) was observed for all compositions. Depending on the parameter chosen to normalize the dose-response curve, the sensitivity range changed. If the initial OSL intensity was chosen as reference, the composition containing 65% B_2O_3 and 15% K_2CO_3 (named L15KB) presented the most intense signal. However, if the total area below the curve was considered, the composition containing 70% B_2O_3 and 10% K_2CO_3 (named L10KB) was the most sensitive. A comparison of the OSL decay for the two quoted compositions, after pre-heating to 200 °C for 10 s prior to the OSL readout, showed a slight change in the decay pattern compared to the absence of pre-heating. The pre-heating treatments also showed the correlation between the shallow traps and the fast component of the OSL decay for L15KB. For all compositions, an increase in dose implied an increase in emitted signal, and no saturation was observed between 0.1 Gy and 7 Gy.

1. Introduction

Designing glass for radiation detection is reportedly an emerging focus of glass science [1]. Optical fiber sensors can be located in hazardous radiation areas for remote monitoring and for reaching difficult-to-access locations. In recent years, different glass compositions have been evaluated for use in luminescent dosimetry [2,3]. In general, these studies focused on measuring high doses of radiation (order of grays to few kilograys) using thermoluminescence (TL). Also in recent years, optically stimulated luminescence (OSL) has gained attention as a dosimetric technique due to some advantages over TL. Both TL and OSL techniques are based on the emission of light by a semiconductor or insulator, after being irradiated and stimulated to induce the recombination of the trapped charge carriers (electrons and holes). The recombination is induced by a controlled heating process for TL whereas for OSL it is induced by an optical stimulation [4,5].

The OSL properties of several glasses have already been investigated [6–9], particular emphasis has been placed on real-time dose monitoring in medical procedures [10,11]. In this application, glass fibers can either serve as light-guide for the signal ("extrinsic sensor") or as both radiation sensor and light-guide ("intrinsic sensor"), enabling more efficient measurements over long distances [12]. Common glasses, such as those based on SiO_2, are not tissue equivalent. A tissue equivalent glass, sensitive to radiation and emitting OSL could be a uniquely good material for dosimetric optical fibers.

Ease of production, relatively low cost, suitability to host luminescent activators, tissue equivalence, and the possibility to use boron-10 and thus detect slow neutron, are some of the advantages of borate glasses for dosimetric purposes. Lithium potassium borate (LKB) glasses have been studied for TL dosimetry by several authors [13–15]. However, their OSL dosimetric characteristics have only been recognized recently [16].

Our research examines the OSL features of lithium potassium borate glass as a function of chemical composition. The OSL signal

* Corresponding author.
E-mail address: joaoviniciusbatista@gmail.com (J.V.B. Valença).

https://doi.org/10.1016/j.jlumin.2018.03.060
Received 30 November 2017; Received in revised form 18 March 2018; Accepted 20 March 2018
Available online 23 March 2018

Table 1
Chemical compositions of the produced glasses. The purity level of the reagents are shown in the parenthesis.

Glasses	Composition (mol%)		
	Li_2CO_3 (> 99%)	B_2O_3 (> 98%)	K_2CO_3 (99%)
L10KB	20	70	10
L15KB	20	65	15
L20KB	20	60	20
L25KB	20	55	25
L30KB	20	50	30

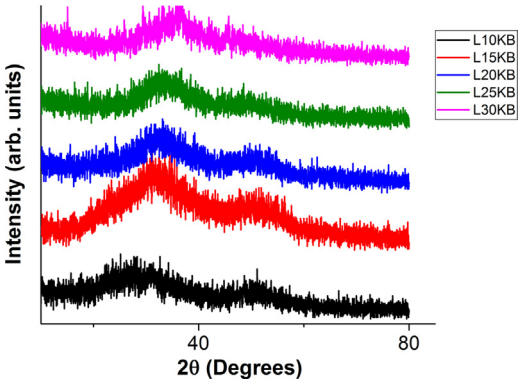

Fig. 1. X-ray diffraction patterns of the LKB glass system.

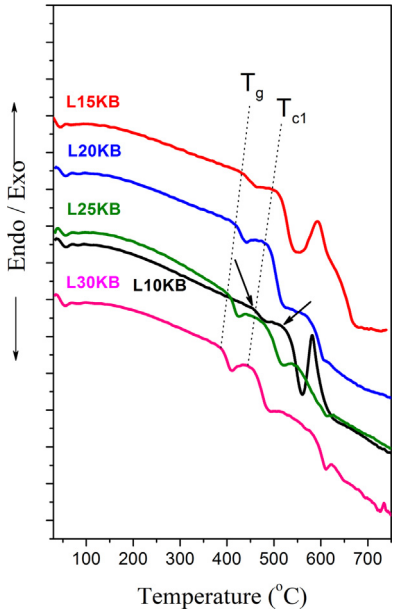

Fig. 2. DTA thermograms of the LKB glass system. Dotted lines and arrows (L10KB) indicate the glass transition temperature (Tg) and a crystallization temperature (Tc1).

Table 2
Glass transition (T_g) and crystallization (T_{c1}) temperatures for each composition [16].

Samples	T_g (± 0.5 °C)	T_{c1} (± 0.5 °C)
L10KB	456.9	481.6
L15KB	432.7	459.1
L20KB	418.4	439.3
L25KB	407.0	422.4
L30KB	394.7	409.5

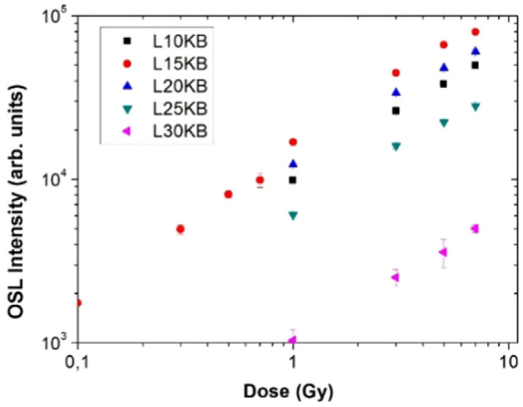

Fig. 3. Dose-response curves of the produced glasses for 1, 3, 5, and 7 Gy. The composition L15KB was also irradiated with 0.1, 0.3, 0.5, and 0.7 Gy. The initial OSL intensity was the chosen parameter in this case.

characteristics are interpreted by combining thermal and optical stimulation of the materials.

2. Materials and methods

Stoichiometric amounts of potassium carbonate (K_2CO_3) and boron oxide (B_2O_3) were added to a fixed 20 mol% amount of lithium carbonate (Li_2CO_3) to produce the LKB glass system with nominal compositions [20% Li_2CO_3 + x% K_2CO_3 + (80 - x)% B_2O_3] with 10 $\leq x \leq$ 30 mol%, (Table 1). All reagents were purchased from Sigma-Aldrich Brazil.

The glasses were produced by melt quenching method. The mixtures of reagents were heated up and kept at 1100 °C for 30 min in a platinum crucible. The cooling process occurred between two 0 °C bronze sheets. After vitrification, the samples were annealed at 350 °C for 24 h to relieve residual internal stresses.

X-ray diffraction (XRD) and differential thermal analysis (DTA) were performed, respectively, using a Rigaku RINT 2000/PC diffractometer (using grains $\leq$ 75 μm and scanning from 10° to 80° at steps of 1°/min) and a Shimadzu DTA-50 differential thermal analyzer (using grains $\leq$ 53 μm, an alumina crucible, a heating rate of 20 °C/min and scanning from 30° to 800°C in a nitrogen atmosphere).

Due to the difficulty to cut them in pieces for the dosimetric tests, glasses were milled and sieved yielding a granulometry between 75 μm and 150 μm. They were then mixed with Teflon in a 3:1 proportion and homogenized. Pellets of 6 mm diameter and 50 mg mass each were achieved by compressing the weighted mixture at 100 kgf/cm^2 for 1 min in a hydraulic press. Twelve pellets were produced for each formulation. In view of improve their mechanical resistance and avoid mass losses during the procedures, a typical thermal treatment of 350 °C for 30 min followed by 400 °C for 90 min was applied. Teflon is well known by its chemical inertness and it presents dosimetric signal only for doses as high as 1 kGy [17].

Irradiation (^{90}Sr/^{90}Y beta particle source – dose rate of 0.1 Gy/s), OSL reading process, and pre-heating procedures were carried out with a Risø TL/OSL reader. The data were recorded right after the irradiations using continuous wave (CW) stimulation. A blue LED with a peak emission at 470 nm (FWHM = 20 nm) was used as the stimulation light. A Hoya U-340 filter (transmission between 290 nm and 390 nm) and an EMI 9235QB photomultiplier tube (maximum quantum efficiency at approximately 200 and 380 nm) were coupled for emitted light detection. For all the OSL measurements, the background signal acquired before an irradiation was subtracted from the signal acquired after each irradiation.

The selection of the pellets for OSL measurements was based on their uniformity and readout reproducibility. At least 3 cycles of irradiation – reading – bleaching, using a dose of 1 Gy (^{90}Sr/^{90}Y beta

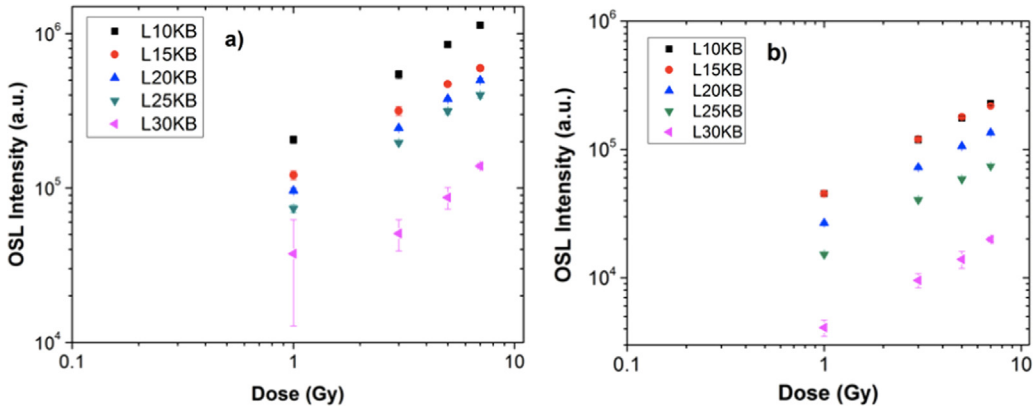

Fig. 4. Dose-response curves considering the area of the OSL decay a) during 40 s of stimulation; b) during 1.28 s of stimulation.

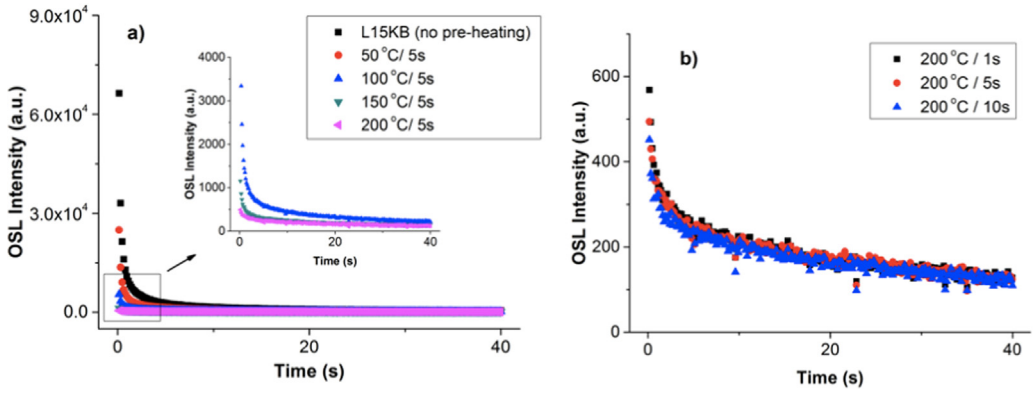

Fig. 5. OSL curves for L15KB with a dose of 5 Gy ($^{90}Sr/^{90}Y$). a) after different pre-heating (the inset shows the OSL decay shape for the higher temperatures); b) after pre-heating of 200 °C during different time intervals.

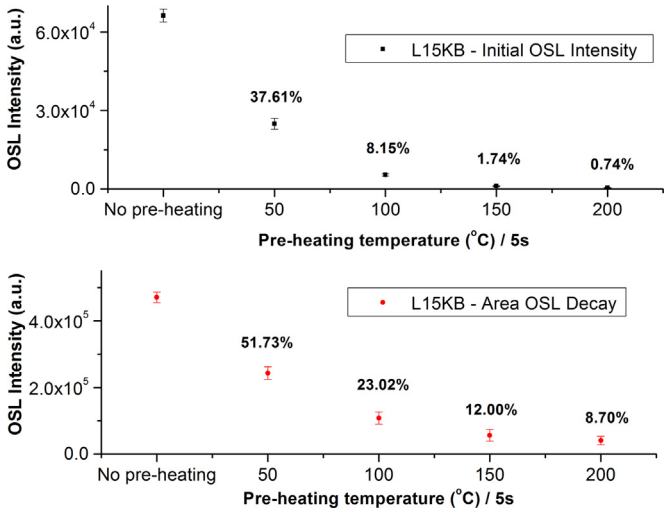

Fig. 6. Percentage of residual value in the initial OSL intensity (graph on the top) and in the area of the OSL decay (40 s stimulation) for L15KB when submitted to different pre-heating treatments. Dose of 5 Gy ($^{90}Sr/^{90}Y$) was used as reference. The temperature in each pre-heating was kept for 5 s.

particle source), were performed. A reading process of 40 s allowed both to acquire the signal and to bleach the samples. Only pellets that presented relative standard deviation lower than 10% were used in the OSL analysis.

Pre-heating treatments using different temperatures and duration were performed in order to observe possible changes in the OSL decay. For these procedures, a dose of 5 Gy ($^{90}Sr/^{90}Y$), a fixed heating rate of 5 °C/s, and the mean of the signal from at least 5 pellets were used. The samples were heated to the chosen pre-heating temperature, kept at it for a few seconds, and finally allowed cooling. The OSL measurements were performed once the system had reached the room temperature again.

3. Results and discussion

3.1. X-ray diffraction and differential thermal analysis

The non-crystalline nature of the samples was easily confirmed with XRD, which showed similar broadband patterns for all compositions (Fig. 1).

The glass transition temperatures (T_g) and the first crystallization temperature (T_{c1}) were determined by DTA analysis [16] (Fig. 2). The transformation of BO_3 triangles in BO_4 tetrahedra, an effect well known as 'Boron Oxide Anomaly' [18], did not occur for this batch, indeed the T_g is constantly decreasing when increasing the amount of potassium carbonate (Table 2).

3.2. Dose-response curves

All 12 pellets produced for each formulation presented a relative standard deviation lower than 10% during the reproducibility test. The same statistical parameter provided values lower than 10% also for the uniformity of each group.

The dose-response curves are shown in Fig. 3, data points are based on the average initial OSL intensity of three different pellets for each dose. The glow curve was obtained during 40 s, however only the initial OSL intensity (number of counts in the first data channel, which corresponds to the initial 0.16 s of measurement) was used in the analysis.

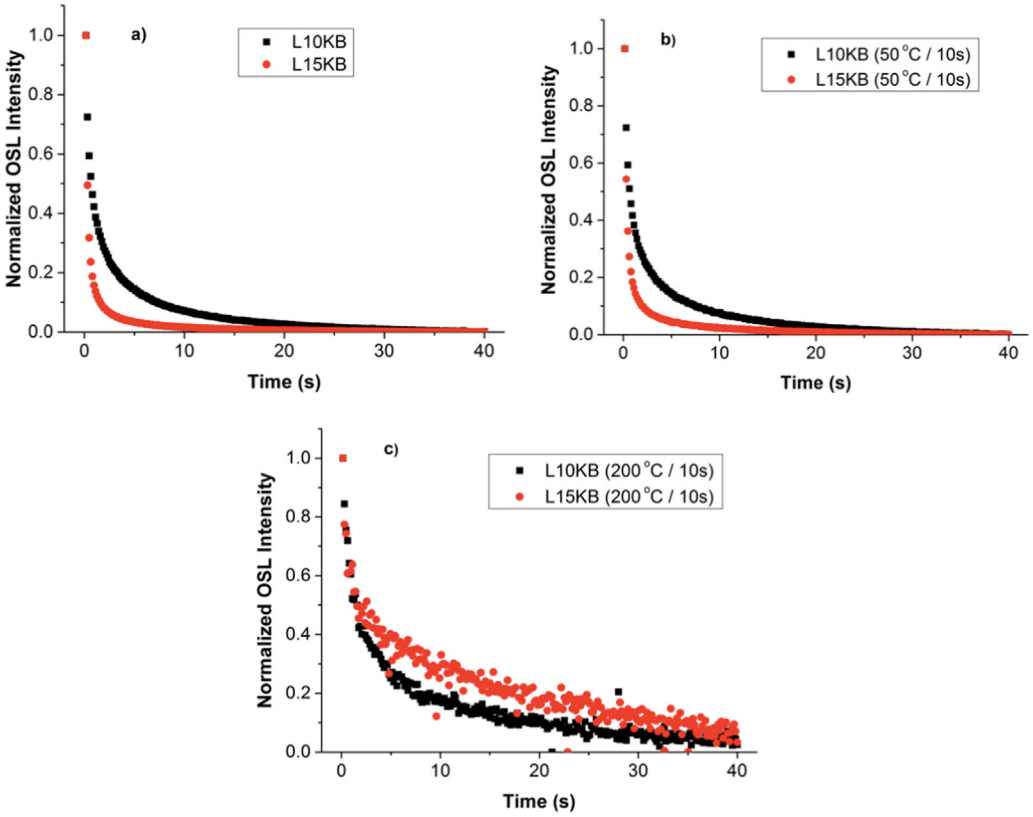

Fig. 7. L10KB and L15KB OSL decay curves with a dose of 5 Gy ($^{90}Sr/^{90}Y$), normalized to their initial intensity. a) Without pre-heating. After a 10 s pre-heating of b) 50 °C and c) 200 °C.

Table 3
OSL parameters for the compositions L10KB and L15KB using the curves with and without pre-heating treatments.

Sample (treatment)	CW-OSL component	Coefficient (A)	Decay constant (s)
L15KB (no annealing) R^2 = 0.99974	Fast	1.35×10^5 (A_1)	0.14 (τ_1)
	Medium	2.03×10^4 (A_2)	0.85 (τ_2)
	Slow	4.28×10^3 (A_3)	6.94 (τ_3)
L15KB (annealed at 200 °C/10 s) R^2 = 0.95370	Fast	2.00×10^2 (A_1)	0.66 (τ_1)
	Slow	1.66×10^2 (A_2)	18.10 (τ_2)
L10KB (no annealing) R^2 = 0.99969	Fast	3.34×10^4 (A_1)	0.22 (τ_1)
	Medium	1.52×10^4 (A_2)	1.62 (τ_2)
	Slow	7.61×10^3 (A_3)	9.54 (τ_3)
L10KB (annealed at 200 °C/10 s) R^2 = 0.98229	Fast	3.01×10^2 (A_1)	0.93 (τ_1)
	Slow	1.73×10^2 (A_2)	10.37 (τ_2)

Since L15KB was the most intense light emitter, measurements for lower doses were also performed with this glass type. The linear fit yielded a coefficient of determination (R^2) of 0.98016.

A concentration quenching seems to be occurring as the signal intensity increases up to a 15% concentration of K_2CO_3 (L15KB) and decreases monotonically for higher concentrations. Considering the total area under the OSL decay curve integrated over 40 s of stimulation, the analysis of the dose-response curves provided a different relation between glass formulations and their responses (Fig. 4a). Further, taking into consideration the area under the OSL decay curve during 1.28 s of stimulation, it is possible to see the inversion in the behavior of the light emission occurring between the batches L10KB and L15KB (Fig. 4b). In Fig. 4b the symbols indicating the OSL intensity of the L10KB and L15KB samples as a dose function are overlapping. No hint of saturation was observed in all cases.

Considering the average of the results for the various doses, L15KB provided 40.83% more signal than L10KB with reference to the initial OSL intensity; conversely, L15KB presented 42.08% less signal than L10KB with reference to the total area of the OSL decay.

Pontuschka et al. [19] reported that, in the absence of impurities, the oxygen vacancies of borate glasses behave as electron traps after irradiation and these traps present an average depth of about 0.2 eV. They also showed that the holes may be trapped in so-called boron-oxygen hole centers (BOHC) with an average energy of 1.0 eV. In our work, the amount of potassium was varied in the lithium borate glasses. Increasing K_2CO_3 and decreasing the amount of boron oxide implies a decreasing number of traps associated with the measured emission wavelengths. This leads to a considerable reduction in the OSL integrated area. For a given photon flux of the stimulation source, a higher photoionization cross-section (σ) of the traps implies a higher probability of releasing trapped electrons, and a higher emission of light through recombination. Therefore, traps with higher photoionization cross-section provided greater value for the initial emission to the L15KB OSL decay in comparison with L10KB.

The OSL signal characteristics of the L10KB and L15KB batches were analyzed with pre-heating treatments of different duration and temperatures. Fig. 5.a shows how the L15KB OSL curve changes with different pre-heating temperatures, keeping the maximum temperature for 5 s. A considerable reduction in OSL signal after the pre-heating treatments is easily noted. However, even after a pre-heating to 200 °C for 10 s (Fig. 5.b) the characteristic decay shape of the CW-OSL curve is still present, meaning that part of the OSL signal derives from deeper traps.

The reduction in OSL intensity of L15KB samples with pre-heating at different temperatures is shown in Fig. 6; the numbers above plotted points represent the percentage of residual value after preheating compared to non-preheated samples. A faster decrease of the initial OSL intensity indicates that the traps with lower activation energy originate the fast decay component of the curve. A similar behavior was already

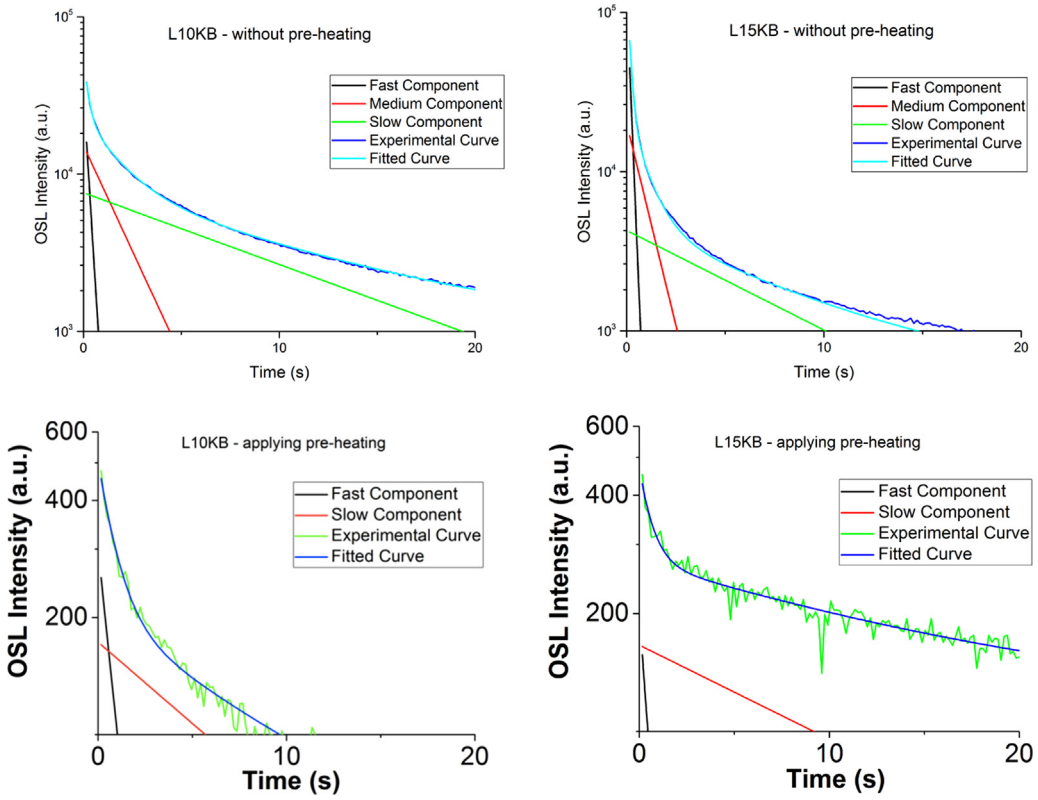

Fig. 8. Fitted curves for the samples L10KB and L15KB without and with pre-heating.

reported for crystalline materials and phosphate glass [7,20].

OSL curves for L10KB and L15KB, both with and without pre-heating, are presented in Fig. 7, where data are normalized to the initial OSL intensity. In the situation with no pre-heating (Fig. 7a) and with pre-heating at 50 °C for 10 s (Fig. 7b), L15KB showed a faster decay than L10KB. For a pre-heating at 200 °C for 10 s, a slight inversion on this behavior can be noted (Fig. 7c).

Table 3 shows the parameters obtained from an exponential fitting of the OSL decay curves presented in Fig. 7. For data without pre-heating, the decays were fitted using a three component exponential function:

$$I_{OSL} = A_1{*}\exp(-t/\tau_1) + A_2{*}\exp(-t/\tau_2) + A_3{*}\exp(-t/\tau_3)$$

where A_1, A_2, and A_3 are constant coefficients, τ_1, τ_2, and τ_3 are the decay constants related to the different sets of traps and I_{OSL} is the OSL intensity.

Experimental and fitted OSL glow curves, as well as their separate exponential terms, are shown in Fig. 8. A good agreement may be observed between applied fitting and experimental result, the faster decay of L15KB without preheating is also clear. With pre-heating at 200 °C for 10 s, an accurate fit may be obtained using only two exponential terms, which implies a variation of the trapped charge distribution. Overall, inspection of the decomposition of the curves in the different exponentials indicates complex phenomena of electron de-trapping and re-trapping which warrants further analysis.

4. Conclusions

The methodology developed in this study allows the efficient production of glasses, confirmed by XRD and DTA analysis. Differences in the dose-response curves of these glasses may be attributed to the different trap distribution, which is significantly influenced by the addition of glass modifiers and glass former. L10KB presented the most intense value of OSL integrated signal for a 40 s stimulation, and its decay pattern was slower in comparison with L15KB. A comparison of the OSL decay for the two quoted compositions, after pre-heating to 200 °C for 10 s prior to the OSL readout, showed a slight change in the decay pattern compared to the absence of pre-heating. The pre-heating treatments showed that traps with lower activation energy originate form the fast decay component of the OSL signal for L15KB. For all compositions, an increase in dose implied an increase in emitted signal, and no saturation was observed between 0.1 Gy and 7 Gy. A complete analysis of this type of characteristics will help choosing the best formulation of luminescent glass for each specific application.

Acknowledgements

This work was supported in part by the Brazilian agencies CNPq, FAPITEC-SE, CAPES, FAPEMIG, and by the Instituto Nacional de Metrologia das Radiações na Medicina (INCT).

References

[1] J.C. Mauro, C.S. Philip, D.J. Vaughn, M.S. Pambianchi, Glass science in the United States: current status and future directions, Int. J. Appl. Glass Sci. 5 (2014) 2–15.
[2] M.M. Elkholy, Thermoluminescence of B_2O_3-Li_2O glass system doped with MgO, J. Lumin. 130 (2010) 1880–1892.
[3] W.E.F. Ayta, V.A. Silva, N.O. Dantas, Thermoluminescent properties of a Li_2O–B_2O_3–Al_2O_3 glass system doped with CaF_2 and Mn, J. Lumin. 130 (2010) 1032–1035.
[4] S.W.S. McKeever, M. Moscovitch, Topics under debate-on the advantages and disadvantages of optically stimulated luminescence dosimetry and thermoluminescence dosimetry, Radiat. Prot. Dosim. 104 (2003) 263–270.
[5] E.G. Yukihara, S.W.S. McKeever, Optically Stimulated Luminescence – Fundamentals and Applications, First ed., John Wiley & Sons, United Kingdom, 2011.
[6] J. Qiu, Y. Shimizugawa, Y. Iwabuchi, K. Hirao, Photostimulated luminescence of Ce 3+ -doped alkali borate glasses, Appl. Phys. Lett. 71 (1997) 43–45.
[7] A. Timar-Gabor, C. Ivascu, S. Vasiliniuc, L. Daraban, I. Ardelean, C. Cosma, O. Cozar, Thermoluminescence and optically stimulated luminescence properties of the $0.5P_2O_5$-xBaO-(0.5-x)Li_2O glass systems, Appl. Radiat. Isot. 69 (2011) 780–784.
[8] C.A.G. Kalnins, H.E. Heidepriem, N.A. Spooner, T.M. Monro, Optically stimulated luminescence in fluoride-phosphate glass for radiation dosimetry, J. Am. Ceram.

Soc. 94 (2011) 474–477.
[9] H. Nanto, R. Nakagawa, Y. Takei, K. Hirasawa, Y. Miyamoto, H. Masai, T. Kurobori, T. Yanagida, Y. Fujimoto, Optically stimulated luminescence in x-ray irradiated xSnO-(25-x)SrO-75B_2O_3 glass, Nucl. Instrum. Methods Phys. Res. A 784 (2015) 14–16.
[10] S. O'Keeffe, C. Fitzpatrick, E. Lewis, A.I. Al-Shamma'a, A review of optical fibre radiation dosimeters, Sens. Rev. 28 (2008) 136–142.
[11] A.L. Huston, B.L. Justus, P.L. Falkenstein, R.W. Miller, H. Ning, R. Altemus, Optically stimulated luminescent glass optical fibre dosemeter, Radiat. Prot. Dosim. 101 (2002) 23–26.
[12] C.A.G. Kalnius, H.E. Heidepriem, N.A. Spooner, T.M. Monro, Radiation dosimetry using optically stimulated luminescence in fluoride phosphate optical fibres, Opt. Mater. Express 2 (2012) 62–70.
[13] Y.S.M. Alajerami, S. Hashim, A.T. Ramli, M.A. Saleh, T. Kadni, Thermoluminescence characteristics of the Li_2CO_3-K_2CO_3-H_3BO_3 glass system co-doped with CuO and MgO, J. Lumin. 143 (2013) 1–4.
[14] Y.S.M. Alajerami, S. Hashim, S.K. Ghoshal, M.A. Saleh, T. Kadni, M.I. Saripan, K. Alzimami, Z. Ibrahim, D.A. Bradley, The effect of TiO2 and MgO on the thermoluminescence properties of a Lithium Potassium Borate glass system, J. Phys. Chem. Solids 74 (2013) 1816–1822.
[15] S. Hashim, Y.S.M. Alajerami, A.T. Ramli, S.K. Ghoshal, M.A. Saleh, A.B. Abdul Kadir, M.I. Saripan, K. Alzimami, D.A. Bradley, M.H.A. Mhareb, Thermoluminescence dosimetry properties and kinetic parameters of lithium potassium borate glass co-doped with titanium and magnesium oxides, Appl. Radiat. Isot. 91 (2014) 126–130.
[16] J.V.B. Valença, I.S. Silveira, A.C.A. Silva, N.O. Dantas, P.L. Antonio, L.V.E. Caldas, F. d'Errico, S.O. Souza, Optically stimulated luminescence of borate glasses containing magnesia, quicklime, lithium and potassium carbonates, Rad. Phys. Chem. 140 (2017) 83–86.
[17] R.A.P.O. D'Amorim, M.I. Teixeira, S.O. Souza, J.M. Sasaki, L.V.E. Caldas, Influence of Teflon® agglutinator on TLD spodumene pellets, J. Lumin. 132 (2012) 266–269.
[18] Y.D. Yiannopoulos, G.D. Chryssikos, E.I. Kamitsos, Structure and properties of alkaline earth borate glasses, Phys. Chem. Glass 42 (2001) 164–172.
[19] W.M. Pontuschka, L.S. Kanashiro, L.C. Courrol, Luminescence mechanisms for borate glasses: the role of local structural units, Glass Phys. Chem. 27 (2001) 37–47.
[20] R.A. Barve, R.R. Patil, S.V. Moharil, B.C. Bhatt, M.S. Kulkarni, Optically stimulated luminescence in Cu^+ doped lithium orthophosphate, Phys. B: Condens. Matter 458 (2015) 117–123.